Optical and Quantum Electronics (2024) 56:784
https://doi.org/10.1007/s11082-024-06596-0

Synthesis, optical, and spectroscopic studies of bismuth boro-tellurite glass system containing BaO and V_2O_5

B. Srinivas[1] · Khadijah Mohammedsaleh Katubi[2] · Ashok Bhogi[1] · Sheik Ahammed[3,4] · T. V. Surendra[4] · Abdul Hameed[5] · Md. Shareefuddin[6] · M. S. Al-Buriahi[7]

Received: 11 November 2023 / Accepted: 7 February 2024 / Published online: 25 March 2024

Abstract

A melt quenching technique was used for the preparation of xBaO–(30-x)TeO_2–35Bi_2O_3–33B_2O_3–2V_2O_5 ($5 \leq x \leq 25$ mol%) glasses. The structural modifications are studied by X-ray diffraction, DSC, optical, infrared spectroscopy, and Raman as a function of BaO mol%. The progressive incorporation of BaO mol% in the BTBiBV glasses decreases the optical band gap values as the number of free electrons increases with the creation of additional NBOs. The FTIR spectra of the prepared glasses consist of BO_3 trigonal and BO_4 tetrahedral units while TeO_2 changes to TeO_3 andTeO_4 structural units. The Raman spectra shows that the replacement of BaO with TeO_2 decreases the concentration of Te–O–Te linkages within the volume of host glass, which increases the concentration of Ba–O–Te linkages along with BO_3 units. Due to this, the overall glass formers connectivity decreases which intern to the creation of NBOs. Moreover, the research highlighted that BTBiBV-5 glasses have exceptional optical properties making them promising materials for photonics, optoelectronics, and optical communication device applications.

Keywords FTIR · Raman · Oxide glasses · Non-bridging oxygen ions

✉ M. S. Al-Buriahi
mohammed.al-buriahi@ogr.sakarya.edu.tr

[1] Department of Physics, VNR Vignana Jyothi Institute of Engineering and Technology, Hyderabad, Telangana 500090, India

[2] Department of Chemistry, College of Science, Princess Nourah bint Abdulrahman University, P.O. Box 84428, 11671 Riyadh, Saudi Arabia

[3] CVR College of Engineering, Ibrahim Patnam, Telangana 501510, India

[4] Department of Chemistry, Chaitanya Bharathi Institute of Technology (A), Hyderabad, Telangana 500075, India

[5] Department of Physics, University College for Women, Osmania University, Hyderabad, Telangana 500095, India

[6] Department of Physics, Osmania University, Hyderabad, Telangana State 500007, India

[7] Department of Physics, Sakarya University, Sakarya, Turkey

1 Introduction

In general, the chemical composition of glasses primarily governs their physical, thermal, electrical, and spectroscopic properties, with the structural arrangement also exerting a notable influence on these attributes. The selection of glass composition is often a compromise among several elements and is determined by the application of the glasses (for example, lasers or optical amplifiers).The structure of the glasses is critical in identifying the significant technological applications in terms of structure-related properties, which leads to the fabrication of new types of materials (Hall et al. 1989; Elbatal et al. 2014; Fernández Navarro et al. 2013). The variation of the host glass network that takes place in bismuth-borate glasses because of the adding of some alkali (Li_2O, Na_2O, K_2O) and some alkaline (MgO, CaO, SrO, BaO) produces a variety of various non-linear optical characteristics that make these glasses appropriate for use in optoelectronic applications (Al-Harbi et al. 2021; Shamshad et al. 2017; Marzouk et al. 2013; Walia and Singh 2021; Altowyan et al. 2021; Stalin et al. 2021; Vedeanu et al. 2012). When compared to the extensive research into alkali bismuth-borate glasses, considerably less attention was devoted by researchers than was dedicated to the study of alkali bismuth-borate glasses for applications as rapid ion conductors.

The presence of high polarizable Bi^{3+} ions and an asymmetry in the oxygen coordination polyhedra of these ions has been shown to facilitate the non-crystallization of melts (Srinivas et al. 2018a). Whereas covalently bonded B_2O_3 is a very effective glass-forming material that has fascinating chemical and physical features. Insulating properties are inherent to B_2O_3 glasses, and the B^{3+} ion coordinates with oxygen atoms to create BO_3 or BO_4 units. B_2O_3 glasses have a fundamentally insulating composition. Borate glass is the material of choice for optical applications due to its excellent transparency, low-melting point, and good thermal-stability (Srinivas et al. 2022a, 2020; Richards et al. 2010).

Tellurite-based glasses are transparent in the near- and mid-infrared range and have low T_g values, high moisture resistance, good mechanical strength, excellent chemical resilience, and low phonon energy (Richards et al. 2013). Additionally, these glasses have a large third-order nonlinear optical susceptibility and high refractive indices. Due to their exceptional optical and electrical characteristics, tellurite-based glassy systems have the potential to be used in a variety of applications, notably in the fields of microelectronics and opto-acoustics (Jambhale and Chanshetti 2018). The functioning of glasses may be improved for the optical, electrical, and magnetic applications that are required by adding transition metal oxides such as CuO, MnO_2, Cr_2O_3, V_2O_5, etc. (Srinivas et al. 2019, 2021, 2022b, c, ; Bhogi and Kistaiah 2015; Bhogi et al. 2022a, 2022b; Lalithaphani et al. 2018). In particular, V_2O_5 has fascinating optoelectronic properties and possesses the capacity to govern phase separation in glasses. In addition to this, V_2O_5 has the potential to act as both a former and a modifier when it is combined with glass formers (Abdelghany and ElBatal 2016; Ghoneim et al. 2011).

The deep perception of the structure can be provided by the coordination number of the metal ions corresponding to neighboring oxygen ions. The metal ion vibrations are more active in the IR region which makes Infrared (IR) spectroscopy an efficient technique along with Raman spectroscopy to study the structure of the material. The incorporation of modifier metal ions into the base glasses changes the internal structure and oxygen-bonding nature with the metal ions (Bhogi et al. 2022b; Abdelghany and Hammad 2015; Srinivas et al. 2018b). From the results of modifier ions containing glass studies, it was confirmed that the presence of alkaline earth ions alters the local dynamics of the other neighboring

metal ions (Hameed et al. 2015). The field strength of metal ions varies with metal–oxygen interaction (Montemore et al. 2017). Barium-bismuth-boro-tellurite glasses containing vanadium oxides are prominent glass materials due to their interesting structural properties and also their adequateness in optoelectronic, memory switching, optical communication, and luminescent host materials (Lafi 2016; Srinivas et al. 2015; Ahammed et al. 2022).

This study seeks to examine the fundamental properties of barium-bismuth-boro-tellurite-containing V_2O_5 (xBaO–(30-x)TeO_2–35Bi_2O_3–33B_2O_3–2V_2O_5) glasses. Optical, thermal, FTIR and Raman spectral analysis methods were used in the study to find out how the vanadium ions change the optical and vibrational properties of these glasses. These data establish a correlation between the rise in barium content and the alterations in the structure of these glasses.

2 Experimental

Glasses with the composition (Table 1) xBaO–(30-x)TeO_2–35Bi_2O_3–33B_2O_3–2V_2O_5 ($5 \leq x \leq 25$ mol%) labeled with BTBiBV-1 (5 mol%), BTBiBV-2 (10 mol%), BTBiBV-3 (15 mol%), BTBiBV-4 (20 mol%), BTBiBV-5 (25 mol%) were synthesized by well-known melt-quenching process with the high pure reagents. AR grade reagents such as $BaCO_3$ (Merck-99.98%), TeO_2 (Merck ≥ 99%), Bi_2O_3 (Merck-99.999%), H_3BO_3 (Merck-99.99%), and V_2O_5 (Merck- ≥ 98%) were employed as the starting ingredients. Utilizing a digital electronic balance, the powdered chemicals in each batch were given a weight of 10 gm weighed according to their composition expressed as a percentage of mols. In an agate pestle and mortar, the measured chemicals were pulverized and combined consistently for a period of four hours. Pulverizing the chemicals helps to achieve a more homogeneous mixture, ensuring that the final glass sample has consistent properties. Combining them for four hours allows for sufficient time for the different components to react and form a well-mixed glass precursor. This step is crucial in obtaining accurate and reliable results during subsequent testing and analysis. After obtaining this mixture, it was melted in an electrical muffle furnace at a temperature of 1373 °C for 45 min. To achieve a fine homogeneity, the molten substance was agitated at regular intervals. Finally, the melt was rapidly cooled to 350 °C in the middle of two plates made of stainless steel, which resulted in the preparation of glass samples in the shape of round discs.

At room temperature (RT) in the 20°–80° range with a scan rate of 2° per minute, XRD data was obtained for fine powdered glass samples using a Philips Xpert Pro X-ray diffractometer. Both the source and the detectors, which consisted of a high-speed Si strip detector, were Cu k_α radiations operating at 40 kV and 15 mA. DSC measurements of the

Table 1 Composition of xBaO–(30-x)TeO_2–35Bi_2O_3–33B_2O_3–2V_2O_5 glasses

S. no.	Glass composition	Glass Code	T_g (°C)
1	5BaO–25TeO_2–35Bi_2O_3–33B_2O_3–2V_2O_5	BTBiBV-1	426
2	10BaO–20TeO_2–35Bi_2O_3–33B_2O_3–2V_2O_5	BTBiBV-2	418
3	15BaO–15TeO_2–35Bi_2O_3–33B_2O_3–2V_2O_5	BTBiBV-3	427
4	20BaO–10TeO_2–35Bi_2O_3–33B_2O_3–2V_2O_5	BTBiBV-4	426
5	25BaO–5TeO_2–35Bi_2O_3–33B_2O_3–2V_2O_5	BTBiBV-5	424

present glasses were achieved at 200–600 degrees Celsius on a thermal analyzer made by Perkin Elmer STA 6000. To record the DSC thermographs, the rate of heating was set at 10 degrees Celsius per minute, and the flow rate of nitrogen was set at 100 ml per minute. Pyris, the thermal analysis software that came packaged with STA 6000, was used to carry out an exhaustive data analysis as well as smoothen the data. The thickness of the samples varied anywhere between 0.8 and 1.5 mm. The spectral measurements were conducted employoing a UV–visible spectrophotometer, at room temperature, in a wavelength range of 200–1000 nm on a JASCO V 570 UV–visible spectrophotometer. The glass samples were subjected to infrared transmittance spectroscopy at room temperature using a Perkin Elmer Frontier FTIR instrument that operated within the mid-infrared range of 250–4000 cm^{-1}. The KBr pellet method was used to record FTIR spectra. All the BTBiBV samples underwent a powdering process using 0.2 g of KBr, with a ratio of 2:100, and then it was placed in a 13 mm dye and run through a hydraulic press at a pressure of 7–10 tonnes to produce translucent pallets with an approximate thickness of 1 mm. With the assistance of the spectrum 10 software, the background noise was eliminated, and the baseline was adjusted. The Raman spectra within the range of 50–1600 cm^{-1} were acquired using the Jobin Yvon Horiba LABRAM-HR Raman spectrometer.

3 Results and discussion

3.1 XRD

Figure 1 depicts the XRD features of the BTBiBV glasses, which were obtained by measuring the scattering angles ranging from 10° to 80°. The scattering angles in the XRD pattern represent the diffraction of X-rays by the atoms in the glass structure. In crystalline materials, these diffractions occur at specific angles, resulting in sharp peaks in the XRD pattern. However, in amorphous materials like glass, there is no long-range order of atoms, causing the diffractions to be spread out continuously. This broadening of scattering angles is what gives rise to the broadband or broad hump observed in the XRD pattern of glass samples. Figure 1 demonstrated that the intensity of the broad hump decreased with the composition of the glasses. Adding BaO can influence the packing density and interatomic distances within the glass network. This, in turn, can affect the overall scattering of X-rays and potentially contribute to the observed changes in the broad hump intensity. Which concludes that some disorder had been created and added more evidence that the prepared glass was amorphous in nature (Marzouk et al. 2016; Hameed et al. 2021).

3.2 Physical studies

The density (ρ), as well as other similar parameters such as molar volume (V_m), and boron-boron separation ($d_{B–B}$) of the glass constituents are significant factors in the examination of the glass network and its structural modifications. The density value, which is closely connected to the structural coordination number, provides a visual representation of the consequent structural changes due to vitreous glass structures. Structural compacting occurs when the modifiers are integrated into the host matrix, which can be observed by the density value. Table 2 is an overview of the physical properties of multi component glasses that have been measured and that have been doped with VO^{2+}. The development of nonbridging oxygen inside the glass matrix resulted in certain peculiar modifications to the

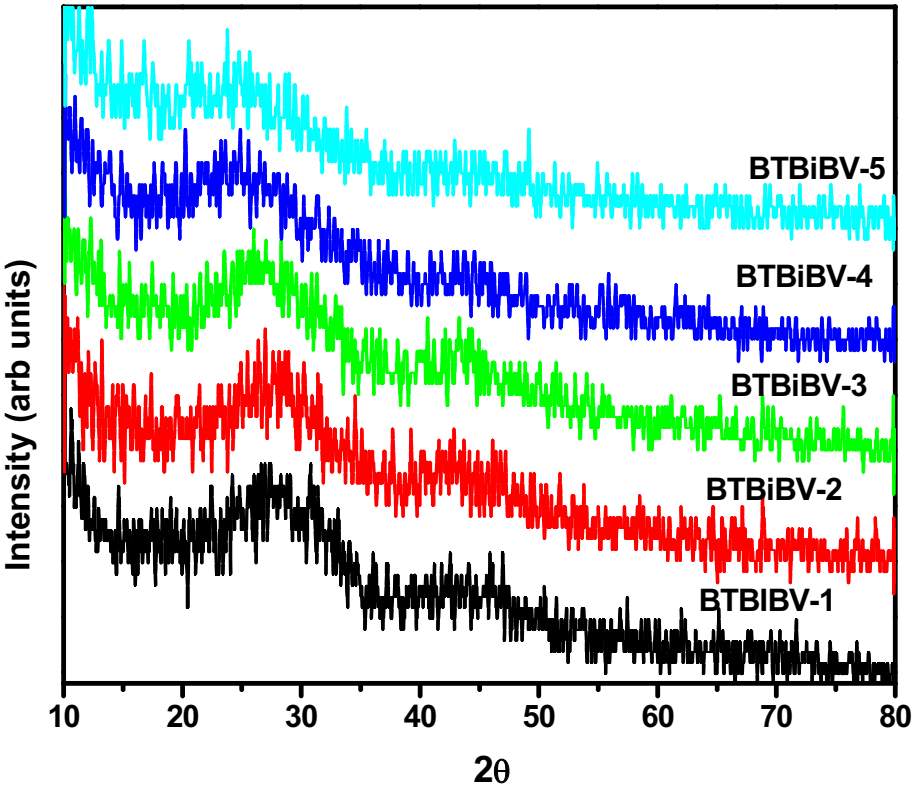

Fig. 1 XRD spectra of $xBaO–(30-x)TeO_2–35Bi_2O_3–33B_2O_3–2V_2O_5$ glasses

Table 2 Summary of data of various physical parameters of $xBaO–(30-x)TeO_2–35Bi_2O_3–33B_2O_3–2V_2O_5$ glasses

Physical parameters	Glass code				
	BTBiBV-1	BTBiBV-2	BTBiBV-3	BTBiBV-4	BTBiBV-5
Density (g/cc)	5.63	5.78	6.23	6.53	6.59
Molar volume (cc/mol)	45.31	44.08	40.85	38.92	38.52
OPD (g atm/l)	59.37	59.89	63.41	65.26	64.64
B–B bond length (Å)	3.83	3.79	3.70	3.64	3.63
Bi–Bi bond length (Å)	3.87	3.83	3.74	3.68	3.66
Opticalbasicity	0.455	0.469	0.484	0.498	0.513
Interaction parameter	0.150	0.148	0.147	0.145	0.144
Ion concentration(10^{22}/cc)	2.66	2.73	2.95	3.09	3.13
Inter ionic distance (Å)	3.35	3.32	3.24	3.19	3.17
Polaron radius (Å)	1.35	1.34	1.31	1.29	1.28
Field strength (10^{22}/cm^2)	1.09	1.11	1.17	1.21	1.22

molar volume trend, which can be shown in Fig. 2. It is well known that the V_m is used to investigate the distribution of oxygen inside the structure of the glass; to put it another way, the molar volume (V_m) of the glass system is affected by the presence of non-bridging oxygen (NBO) species created in the glass structure. The introduction of the modifiers induced the expansion of the glass structure, which was dependent on the presence of bridging oxygens. The following expression has been used to determine the density values (Hameed et al. 2021)

$$\rho = \left(\frac{w_{air}}{w_{air} - w_{xylene}} \times 0.865 \right) \tag{1}$$

$$V_m = \frac{\sum x_i M_i}{\rho} \tag{2}$$

The findings demonstrate a clear relationship between the density values, which range from 5.63 to 6.59 g/cm^3, and the BaO content at the expense of the TeO_2 content. Additionally, the molar volume exhibits a linear decrease, ranging from 45.31 to 38.51 cm^3/mol, as the BaO content increases. Alinear variation is produced as a result of the replacement of light components (TeO_2 density 5.67 g/cm^3) in the glass with heavier ones (BaO density 5.72 g/cm^3).Additionally, present glasses possess densities that lie between the values of pure B_2O_3 (2.46 g/cm^3)and pure Bi_2O_3 (8.9 g/cm.^{3}) (Ahammed et al. 2022). Substituting TeO_2 for BaO is probably responsible for the density change

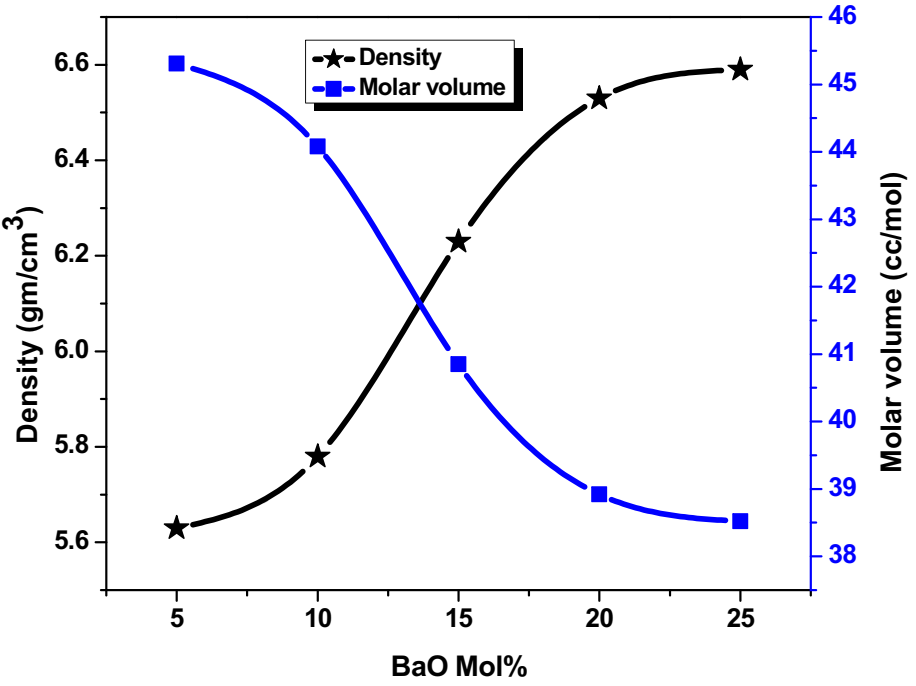

Fig. 2 Variation of molar volume and density with BaO mol%

that happens as a consequence of increasing the modifier. Oxygen packing density (OPD), a measure of how tightly the oxide network is packed, can be calculated from the molecular weight (M_w) and density (ρ) using the following formula (Naresh et al. 2022)

$$\mathrm{OPD} = \left[\frac{\rho}{\mathrm{M_W}}\right] \times \mathrm{n} \tag{3}$$

In the above expression, n represents the number of oxygen atoms in a single unit. The relationship between OPD and BaO concentration is seen in Table 2. It demonstrates that when the concentration of BaO content rises, the OPD increases. This in turn suggests that the structure became tightly packed, and the degree of disorder decreased as the amount of BaO in the material rose. As a result, BaO incorporated into the present glass system results in the development of a more closed macromolecular chain, which in turn increases glass transition temperature.

The boron-boron bond length (d_{B-B}), bismuth-bismuth bond length (d_{Bi-Bi}), and oxygen packing density (OPD) values serve as indicators of the structural compactness and the presence of NBO species within the glass system (Srinivas et al. 2018d; Srinivas et al. 2022a, 2018c). The compactness of the glass structure due to the presence of boric acid and bismuth oxide in considerable amounts can be measured by calculating d_{B-B} and d_{Bi-Bi}. The determination of the boron-boron bond length is achieved by analyzing the volume occupied by a mole of boron atoms within the designated glass structure, as described by the subsequent equation (Srinivas et al. 2018d; Srinivas et al. 2018c)

$$d_{B-B} = \left(\frac{V_m^B}{N_A}\right)^{1/3} \tag{4}$$

where V_m^B and $N_A$represent the molar volume of boron and Avogadro's number respectively. Similarly, the bismuth-bismuth bond length was also calculated. The d_{B-B} and d_{Bi-Bi} values decrease as the concentration of modifier (BaO) increases. It has been observed that $d_{(B-B)}$ and $d_{(Bi-Bi)}$ were reduced, as a result of the presence of the modifiers at higher levels within the disordered glass structure. Table 2 portrays the relationship between the V_m, OPD, d_{B-B}, and d_{Bi-Bi} of the present glass series. It is examined that as V_m decreases OPD increases. The observed variation in OPD provides insights into the distinct packing characteristics of the glass structure. Specifically, the glass network exhibits an open structure that allows for macromolecular chain reactions, while maintaining a rigid configuration. The vanadium ion concentration, denoted by N_i, is of considerable significance because it has a variety of effects on the characteristics of the host material. The formula was used to compute the number of ions that are present in each cubic centimeter as follows (Srinivas et al. 2018a; Srinivas et al. 2022a)

$$N_i = \frac{N_A \times TM(mol\%)}{V_m} \tag{5}$$

where x represents the mole fraction of TM oxide and N_A stands for Avogadro's number. From these findings, the concentration of V-ions grew as the amount of BaO increased. The inter-ionic distance (r_i) and polaron radius (r_p) can be obtained by using the following relations (Vedeanu et al. 2012)

$$r_i = \left(\frac{1}{N_i}\right)^{\frac{1}{3}} \tag{6}$$

$$r_p = \frac{1}{2}\left(\frac{\pi}{6N_i}\right)^{1/3} \tag{7}$$

$$F = \frac{Z}{{r_p}^2} \tag{8}$$

The value of the average TM ion separation, denoted by the symbol (r_p), rises in direct proportion to the amount of BaO in a sample. This is because the structure became closed when BaO was incorporated, and the value of the field strength (F) increases as the amount of BaO increases. This implies that the findings follow the usual behavior, in which the average distance between V and O decreases, resulting in a strong field surrounding the VO^{4+} ions.

3.3 Differential scanning calorimetry (DSC)

To determine the thermal characteristics of the glasses, differential scanning calorimetry (DSC) was carried out. The DSC method is a dynamic approach that may be used for either qualitative or quantitative investigation of the thermal characteristics of a material. It is widely known that the DSC technique is exceptionally well suited for the determination of T_g, T_m and T_c of glasses. Glassy samples are corroborated by the DSC graphs (Fig. 3), which show transition temperatures ranging from 418 to 426 °C (Table 1). When the mole% of BaO increases, the transition temperature varies non-linearly, and as a result, T_m also changes non-linearly.

3.4 Optical studies

The UV–Vis spectra of $xBaO–(30-x)TeO_2–35Bi_2O_3–33B_2O_3–2V_2O_5$ glasses are demonstrated in Fig. 4. As BaO mol% increases, a non-linear change in absorbance is seen. From the standard (Tauc) method, the indirect optical band gap values are measured (Tauc 2012). From Fig. 5, it is identified that the indirect band gap values vary between 2.39 and 2.57 eV. The increase in absorbance (redshift) and the values of optical bandgap are attributed to the incorporation of Ba^{2+} ions, which causes a decrease in the bridging of the free space in the host glass. Mostly, in metal oxide-containing glasses, the maximum valence band comprisesoxygen (*2p*) orbitals, and the minimum conduction band consists of metal (*nS*) orbitals. Comparatively, NBO atoms have greater energies than BO atoms. While breaking the metal–oxygen bonds results in a release of energy, the increase in NBO atoms releases more energy, ultimately reducing the optical band gap (Srinivas et al. 2018d).

The investigation of the optical absorption spectra demonstrates that all samples follow a standard pattern in which a composition-dependent absorption edge is found. The optical absorption edge was found to spread across a broad wavelength range, i.e., there was no sharp edge (Urbach edge), indicating that the prepared glasses were amorphous. The XRD analysis and these findings agree. The strength of the oxygen bonds in the glass-forming

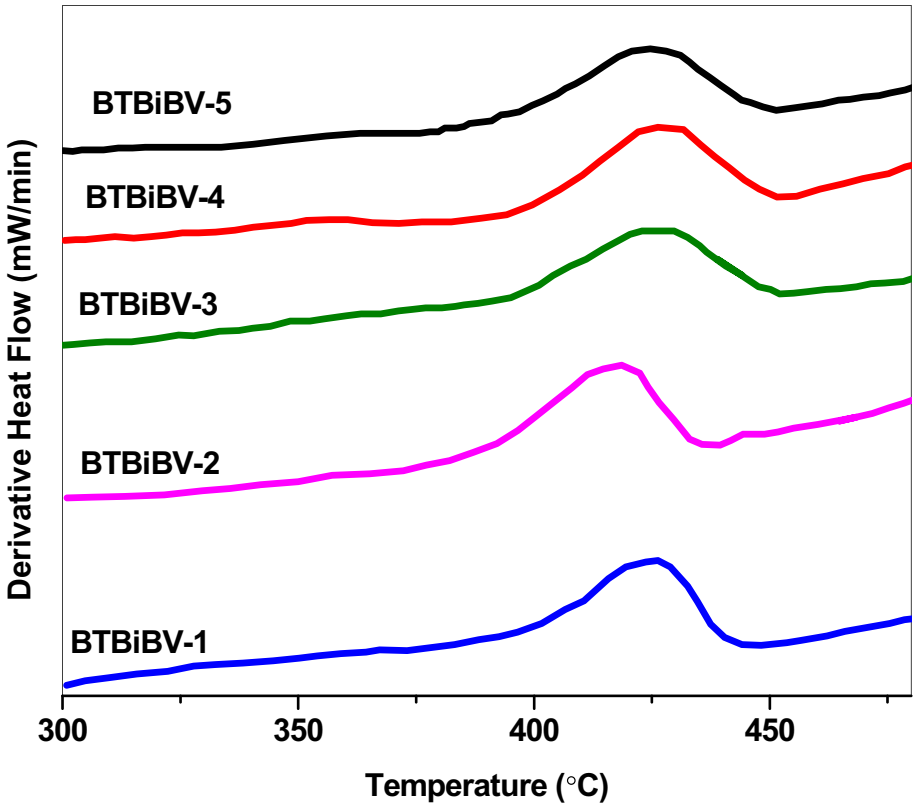

Fig. 3 DSC thermographs of xBaO–(30-x)TeO_2–35Bi_2O_3–33B_2O_3–2V_2O_5 glasses

network is commonly used in estimating the absorption edge. To calculate the absorption coefficient, the following formulais used (Ahamad and Varma 2010)

$$\alpha = \left(\frac{1}{d}\right)\ln\left(\frac{I_0}{I}\right) = 2.303\frac{A}{d} \tag{9}$$

Here, d is the thickness of the samples being analyzed, and I_0 and I are the intensities of the incident and transmitted optical light beams, respectively. The absorbance is given by the formula $\ln\left(\frac{I_0}{I}\right)$. An increase in the absorption coefficient ($\alpha(\omega)$) is the consequence of the electrons jumping from a full band to an empty band because of photon absorption. The quick shift in $\alpha(\upsilon)$ can be represented in terms of the fundamental absorption edge and energy gap. Basic absorption edge and energy gap are two terms used to describe the quick shift in $\alpha(\upsilon)$. According to Davis and Mott, the photon energy of the incident radiation is related to the absorption coefficient $\alpha(\omega)$ as follows (Davis and Mott 1970)

$$\alpha(\upsilon) = \left[B\left(h\upsilon - E_g\right)^n\right]/h\upsilon \tag{10}$$

where B is a constant referred to as the band-tailing parameter. In the case of glass (amorphous) substances, indirect phase transitions are permitted by the Tauc relation (n = 2). From Fig. 5, the E_g values are calculated and presented in Table 3. The well-known Urbach

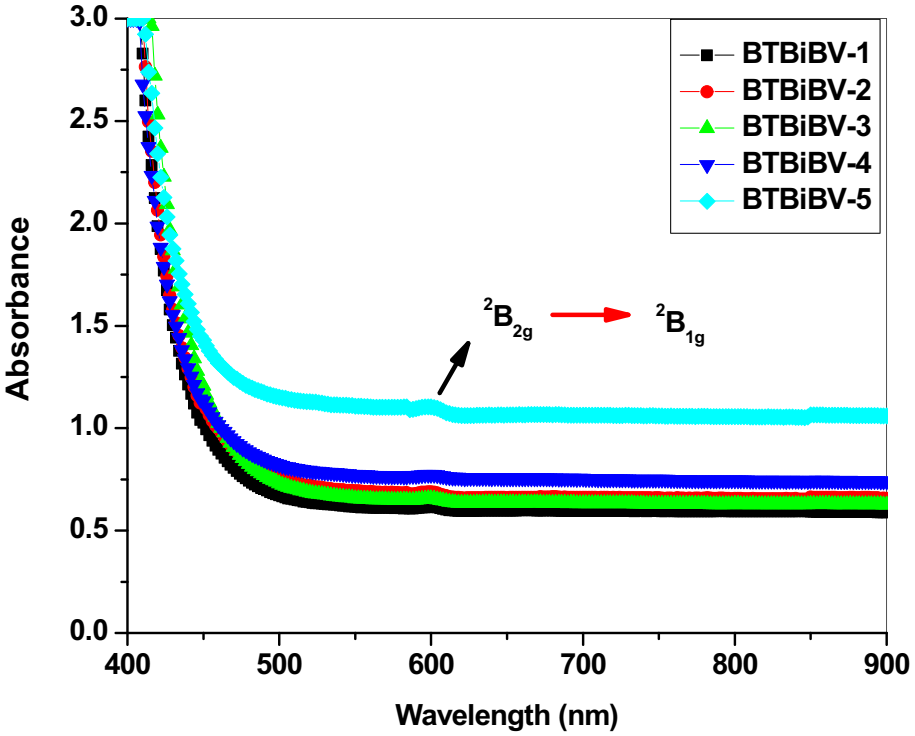

Fig. 4 Optical absorption spectra of xBaO–(30-x)TeO_2–35Bi_2O_3–33B_2O_3–2V_2O_5 glasses

equation establishes the relationship that exists between Urbach energy (ΔE) and absorption coefficient $\alpha(\upsilon)$ (Urbach 1953)

$$\alpha(\upsilon) = \alpha_0 \exp[h\upsilon/\Delta E] \tag{11}$$

where $h\,\upsilon$ is the input photon energy and ΔE is the width of the localized state tail in the bandgap. As an example, Fig. 6 shows the Urbach energy plot. Table 3 lists these values, and it has been discovered that the Urbach energy ΔE decreases in glass samples as the amount of BaO is present in the samples. This may be interpreted as the incorporation of Ba^+ results in a decrease in the disorder of glass systems. Increased BaO concentration causes a decrease in E_g values, which may be explained by the structural changes in the glass network. The introduction of Ba^{2+} ions may disrupt the existing network structure in BTBiBV glasses, causing a decrease in the number of BO_3 units. The incorporation of BaO mol% decreases optical band gap values due to the increase in free electrons and the formation of more non-bridging oxygen (NBO) units. This decrease is attributed to the increased concentration of BaO, which leads to an increase in the number of free electrons within the glass network, ultimately reducing the optical band gap. with the formation of more NBO's.

Optical properties such as the refractive index (n_d), reflection loss (R_L), molar refractivity (R_M), and electronic polarizability (α_m) are essential for glass materials. These values were calculated from the optical band gap measurements. The refractive index

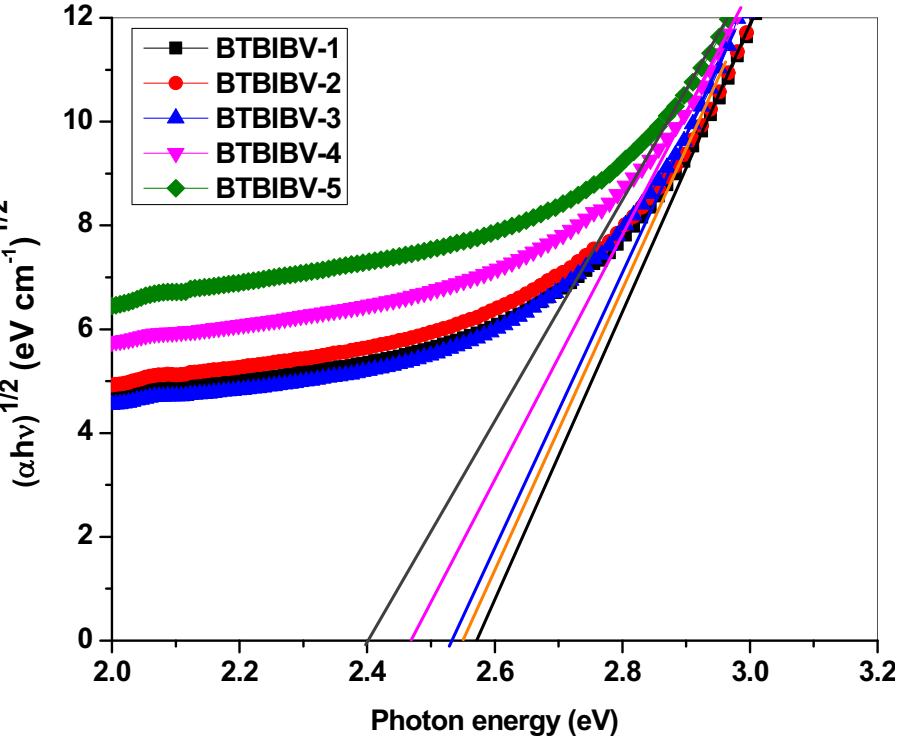

Fig. 5 Tauc's plots of xBaO–(30-x)TeO_2–35Bi_2O_3–33B_2O_3–2V_2O_5 glasses

Table 3 Optical parameters of xBaO–(30-x)TeO_2–35Bi_2O_3–33B_2O_3–2V_2O_5 glasses

Optical parameters	Glass code				
	BTBiBV-1	BTBiBV-2	BTBiBV-3	BTBiBV-4	BTBiBV-5
E_{opt} (eV)	2.57	2.54	2.51	2.46	2.39
Urbach energy (eV)	0.32	0.29	0.25	0.23	0.23
Refractive index	2.52	2.53	2.54	2.56	2.58
Dielectric constant	6.37	6.42	6.47	6.55	6.68
Reflection loss	0.187	0.188	0.190	0.192	0.195
Molar refractivity $(cm)^{-3}$	29.07	28.37	26.38	25.27	25.20
Electronic polarizability($Å^3$)	5.76	5.62	5.23	5.01	5.00
Metallization criteria	0.358	0.356	0.354	0.351	0.346

(n_d) of BTBiBV glasses has been computed by utilizing the following relation (Maalegoundla et al. 2022; Dimitrov and Komatsu 2002)

$$\frac{(n_d^2-1)}{(n_d^2+2)} = 1 - \sqrt{\frac{E_g}{20}} \tag{12}$$

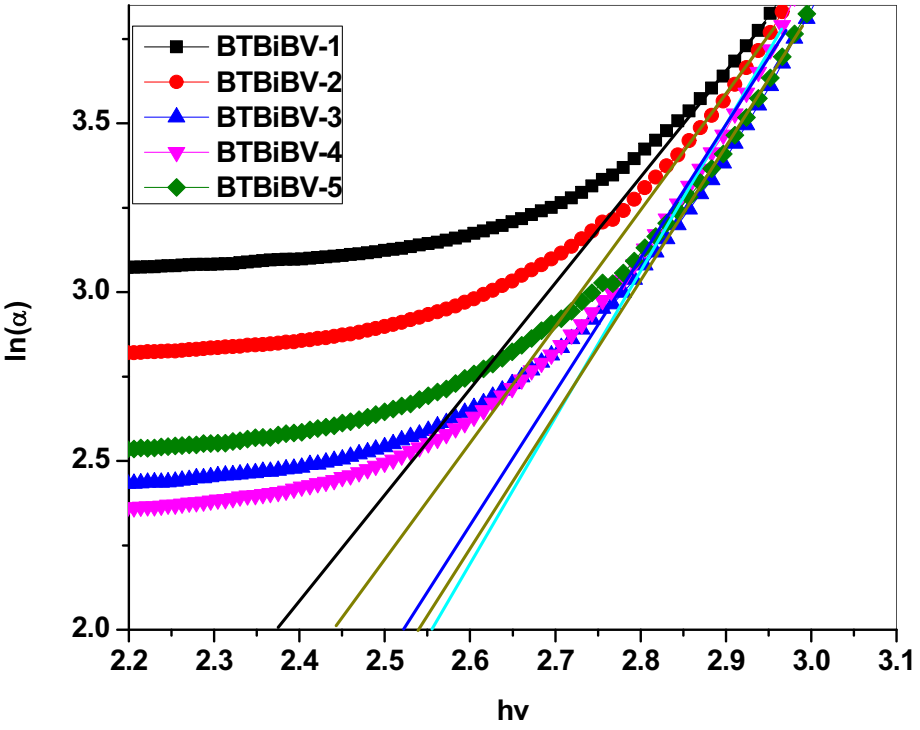

Fig. 6 Urbach plots of xBaO–(30-x)TeO_2–35Bi_2O_3–33B_2O_3–2V_2O_5 glasses

where E_g is the energy band gap. In the present study, the increment observed in a refractive index (n_d) from 2.52 to 2.58 as a result of the rise in the amount of NBOs. From the refractive index (n_d) values the dielectric constant (ε) was calculated by utilizing the formula (Dimitrov and Komatsu 2002)

$$\varepsilon = n_d^2 \tag{13}$$

Molar refractivity is a measurement of a material's total polarizability based on one mole of the substance. The molar refractivity R_M was evaluated using (Dimitrov and Komatsu 2002; Herzfeld 1927)

$$\text{Molar refractivity}\left(R_M\right) = \left[\frac{n_d^2 - 1}{n_d^2 + 2}\right] \times V_m \tag{14}$$

where n_d—refractive index, V_m—molar volume.

Electronic polarizability results from either the propensity for charge dispersal or the displacement of the electron cloud concerning the nucleus that occurs in response to the application of an external electric field.

$$\text{Electronic polarizability}(\alpha_m) = \left(\frac{3}{4\Pi N_A}\right) \times R_m \tag{15}$$

To determine whether prepared glasses are metals or nonmetals, one must use the Metallization criteria (m).

$$\text{Metallization criteria (m)} = \left(1 - \frac{R_m}{V_m}\right) \tag{16}$$

The positive m values observed in all of the BTBiBV glasses indicate that these glasses were not made of metal and exhibit non-metallic behavior, making them insulators.

3.5 FTIR spectra

Infrared spectroscopy is often employed to get the necessary data on the arrangement of the structural units of the prepared glasses. Structures in the glass network are supposed to vibrate independently of one another. In general, well-known stable boron structures are boron triangles and tetraborates. On the other hand, the other stable bismuth configurations are pyramidal and octahedral units. The addition of a metal modifier causes structural changes in the boro-bismuthate glasses. Figure 7 illustrates the IR spectra of xBaO–(30-x) TeO_2–$35Bi_2O_3$–$33B_2O_3$–$2V_2O_5$ glasses. These spectra consist of two prominent absorption peaks located at 770 cm^{-1} and 1500 cm^{-1}. The observed prominent peaks represent the few

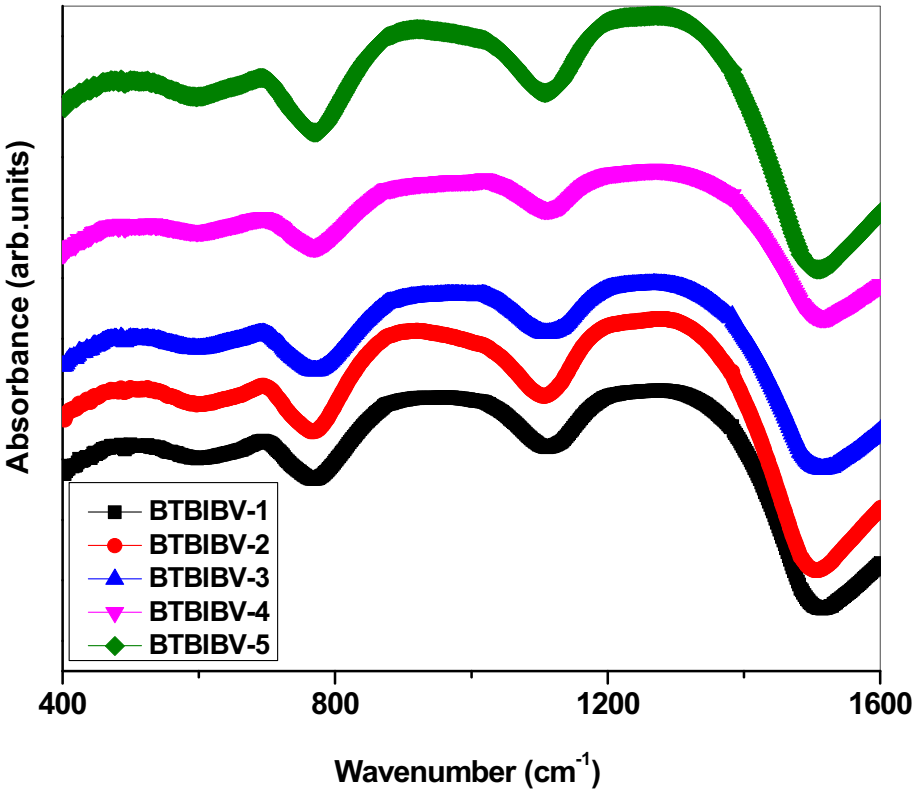

Fig. 7 FTIR spectra of xBaO–(30-x)TeO_2–$35Bi_2O_3$–$33B_2O_3$–$2V_2O_5$ glasses

structural units of the borate network. In addition to these two peaks, there are two more peaks with lower intensity are identified at 470 and 700 cm^{-1}. The band at 470 cm^{-1} is attributed to vibrations of metal cations such as Ba^{2+}, and VO^{2+} ions (Yadav et al. 2013). The deconvolution FTIR spectra for BTBIBV-1 are shown in Fig. 8, and the residual graph for the same is provided in Fig. 9. This graph indicates the degree to which the deconvoluted plot fits the experimental plot, and it can be seen from the graph that the spectrum is completely deconvoluted (Abdelghany 2010, 2013). This indicates that the deconvolution process was successful and accurately separated the overlapping components of the spectrum. The deconvoluted spectrum of BTBiBV-1 is presented in Fig. 8. The extracted broad peaks and their corresponding band assignments of all the BTBiBV are listed in Table 4. The significant absorption band found around 430 cm^{-1} is assigned to the Vibration of metal cations (Ba^{2+}, VO^{2+}) (Yadav et al. 2013). The prominent peak position found in all the glasses around 466 cm^{-1} is due to the vibration of the Bi-O bond in BiO_6 polyhedra (Shaaban et al. 2008; Pascuta et al. 2009). Another prominent band observed around 546 cm^{-1} is attributed to B–O–B bending vibrations (Krishnan et al. 2018). The band at 690–728 cm^{-1} can be related to TeO_3 (tp) trigonal pyramidal units (Suresh et al. 2012). The peak at about 850 cm^{-1} is due to the vibration of the tri, penta, and diborate groups of BO_4 tetrahedra (Kashif et al. 2008). The peaks at 948–978 cm^{-1}can be attributed to stretching vibrations of B-O-Bi linkages (Culea et al. 2009). B–O stretching vibrations of tetrahedral BO_4 units are observed around 1024–1054 cm^{-1}

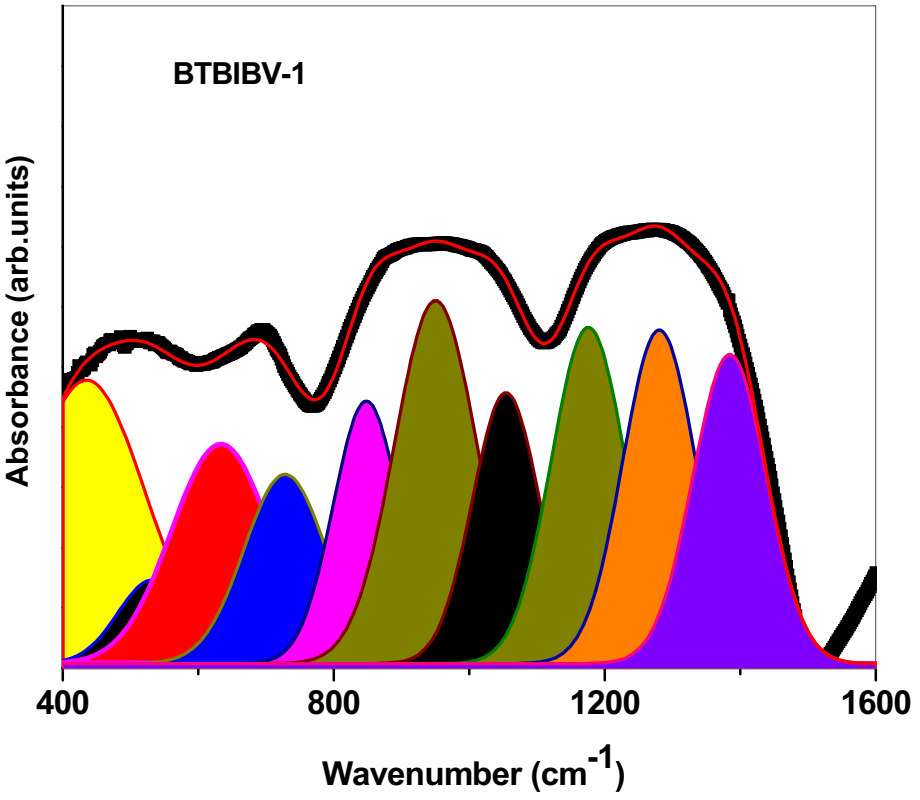

Fig. 8 Deconvoluted FTIR spectra of $5BaO–25TeO_2–35Bi_2O_3–33B_2O_3–2V_2O_5$ glass sample

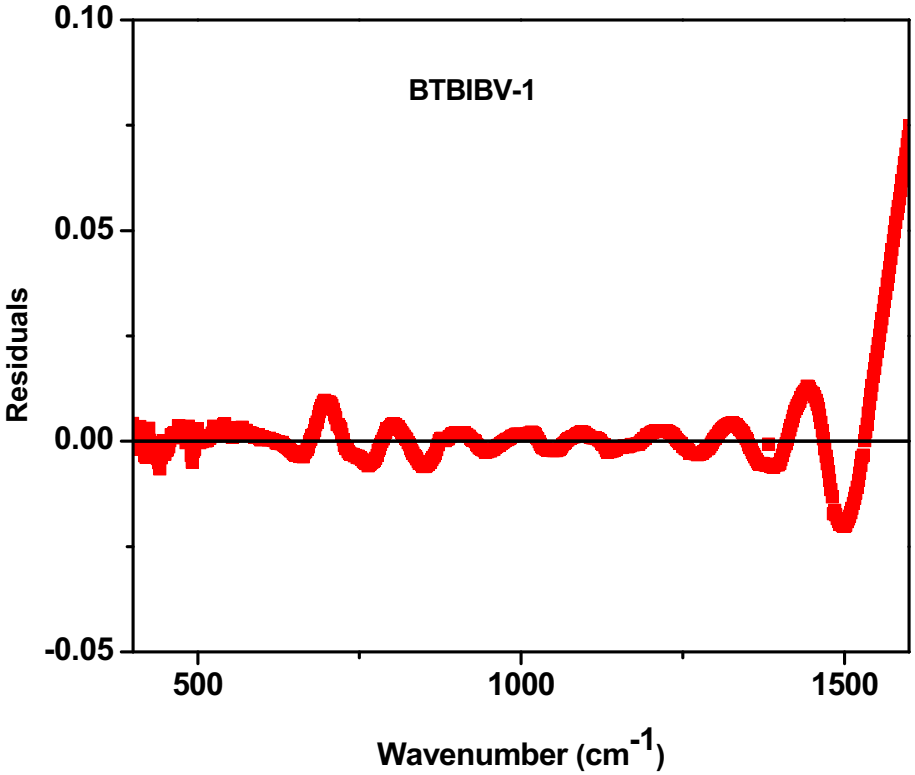

Fig. 9 Residuals graph of $5BaO–25TeO_2–35Bi_2O_3–33B_2O_3–2V_2O_5$ glass sample

wavenumbers (Gautam et al. 2012). The peaks observed between 1173 and 1194 cm^{-1} (Pavani et al. 2011) are shifting to the high-energy region with the addition of BaO assigned to B–O–B vibrations of the varied types of BO_3 groups. Another IR absorption peak around 1260 cm^{-1} is assigned to stretching vibrations of B–O in BO_3 units (Gautam et al. 2012). The presenceof asymmetric stretching modes of BO_3 units is identified at 1305–1312 cm^{-1} (Laorodphan et al. 2016).

By comparing the FTIR spectral areas of BO_4 and BO_3 (containing NBOs), one candetermine how the population of tetrahedral and triangular borate units in the present glasses was affected by BaO. The following equations provide approximations for the number of four-coordinated and three-coordinated boron atoms, respectively (Table 5).

$$N_{BO_4} = \frac{A_{BO_4}}{A_{(BO_4+BO_3)}} \tag{17}$$

$$\text{and} \quad N_{BO_3} = \frac{A_{BO_3}}{A_{(BO_4+BO_3)}} \tag{18}$$

where the areas of the BO_4, BO_3, and BO_3+BO_4 regions in the FTIR spectra are denoted by A_{BO_4}, A_{BO_3} and $A_{(BO_4+BO_3)}$, respectively. Figure 10 depicts the relationship between population variation in BO_4, BO_3, and glass composition. Increasing the BaO mol percent

Table 4 FTIR band assignments of xBaO–(30-x)TeO_2–35Bi_2O_3–33B_2O_3–2V_2O_5 glasses

BTBiBV-1	BTBiBV-2	BTBiBV-3	BTBiBV-4	BTBiBV-5	Band assignment
435	426	441	413	405	Vibration of metal cations (Ba^{2+}) or Bi-O bond in BiO_6 polyhedra
–	483	472	460	506	Bi-O in BiO_6 octahedral unit
633,532	538	546	522	522	B-O-B bonds bending vibrations
728	692	688	695	690	TeO_3 (tp) trigonal pyramidal units
848	895	848	874	873	Vibration of tri, penta and diborate groups of BO_4 units
946	948	950	972	978	Stretching vibrations of B–O–Te, B-O-Bi linkages
1054	1031	1050	1025	1024	B-O stretching vibrations of tetra hedral BO_4groups
1176	1187	1173	1194	1188	B-O-B vibrations of the varied types BO_3 groups
1280	1262	1263	1293	1215	Stretching vibrations of B-O in BO_3 units
1384	1334	1360	1341	1321	B–O stretching vibrations in BO_3 units

Table 5 Raman band assignments of xBaO–(30-x)TeO_2–35Bi_2O_3–33B_2O_3–2V_2O_5 glasses

BTBiBV-1	BTBiBV-2	BTBiBV-3	BTBiBV-4	BTBiBV-5	Band assignment
60	63	62	67	67	β-TeO_2
110	114	114	112	114	Vibration of Bi–O bond in BiO_6 polyhedra or Ba^{2+} vibrations
456	465	466	469	471	Stretching vibrations of Te–O–Te bonds in TeO_4 units
658	665	666	673	684	Asymmetrical stretching of Te–O–Te between TeO_4tbp
770	769	770	774	773	Bending vibration of Te–O along with Ti atoms in TiO_4/TiO_6
803	801	801	–	804	Boroxol ring
931	934	927	906	926	Ortho-borate groups
1232	1244	1263	1285	1270	BO_3 triangular units linked to BO_4 units
1637	1625	1630	1612	1627	Stretching vibrations of BO_3 triangles

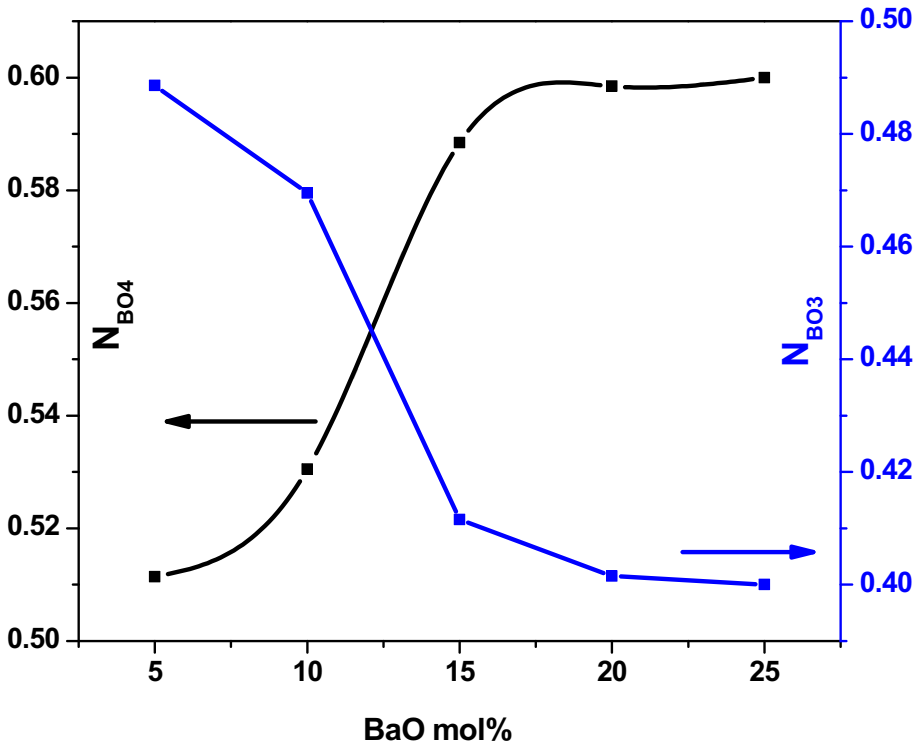

Fig. 10 Population variations of BO_4 and BO_3 with BaO mol%

in the glass composition increases BO_4 population while lowering the BO_3 population, as seen in Fig. 10. Because more NBOs are present in the glass network due to an increase in the BO_4 population, molar volume decreases.

3.6 Raman spectra

Figure 11 shows the room temperature Raman spectra of BTBiBV glasses. The obtained Ramanspectra are classified into two different groups. The first group belongs to below 800 cm^{-1}, which corresponds to the heavy metal ions and the above 800 cm^{-1} is the second group that corresponds to the pure borate networks. The increase of BaO mol% in the present glasses creates more NBOs which results in the conversion of TeO_4 (tbps) to TeO_3 (tps) due to the increased number of NBOs. The presence of β-TeO_2 is confirmed by the observed peak at 63 cm^{-1} (Yadav and Singh 2015). The band centered at 114 cm^{-1} can be attributed to thevibrations of superimposed metal cations Bi^{3+} in BiO_6/V^{4+} in VO_6 units along with thevibrations of Ba^{2+} ions (Majhi et al. 2013). With a rising percentage of BaO mol% in the glass host matrix, the peak at 465 cm^{-1} shifts to higher energy and becomes more intense, suggesting that it is caused by the stretching and bending vibrations of oxygen in Te–O–Te links in TeO_4 units (Kundu et al. 2014). The peak observed around 770 cm^{-1} in all the glasses was attributed to the bending vibration of the Te–O bond along with Ti atoms in TiO_4/TiO_6 structural units. The presence of a Boroxol ring is observed at 804 cm^{-1} in all the glasses except the BTBiBV-4 glass sample. The peak appearing at

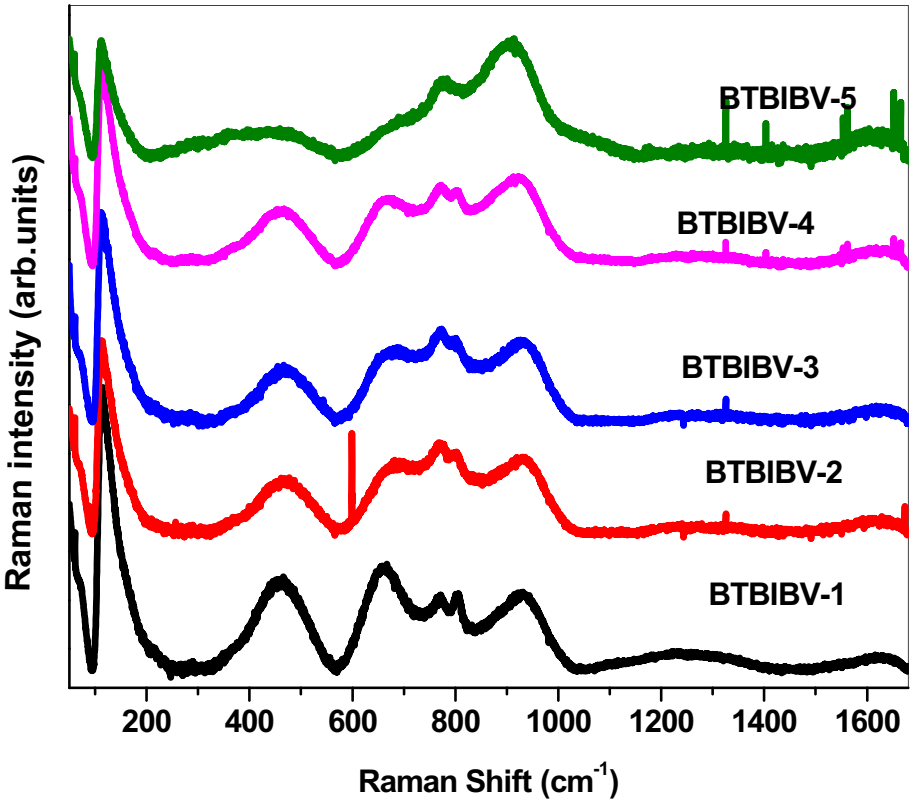

Fig. 11 Raman spectra of $xBaO–(30-x)TeO_2–35Bi_2O_3–33B_2O_3–2V_2O_5$ glasses

934 cm^{-1} indicates the presence of B–O–B and B–O vibrational modes in ortho-borate groups of BO_3 units. The 934 cm^{-1} peak has been found to shift towards the lower wave number side when BaO concentration rises. A rise in BO_3 creation might be the cause. The band between 1230 and 1285 cm^{-1} is an indication of the combined vibration response of B–O in BO_3 and B–O stretching vibrations involving NBOs in pyro borate units. Raman peaks of stretching vibrations of BO_3 triangles are positioned at 1630 cm^{-1}.

4 Conclusions

High-quality alkaline earth oxide-based bismuth boro tellurite glasses were synthesized using the melt quenching method, to thoroughly examine their physical, structural, thermal, and optical properties. By using X-ray diffraction patterns, it was discovered that all the glasses were amorphous and homogenous in nature. Thermal analyses showed that the glass transition temperature (T_g) of these glasses was observed to be between 418 and 426 °C. The optical absorption spectra showed a single and broad peak with an Urbach tail, and the density was found to be 5.63–6.59 g/cm^3. The Optical absorption spectra of present glasses are evident ($^2B_{2g} \rightarrow {}^2B_{1g}$ transition) for the presence of vanadium ions asvanadyl (VO^{2+}) ions. The progressive incorporation of BaO mol% in the BTBiBV glasses

decreases the optical band gap values due to the increase of the number of free electrons with the formation of more NBOs. These glasses were found to have a lower refractive index of 2.52 and showed good optical transparency in the visible and near-infrared regions of the spectrum. Various functional and molecular units were discovered in the FTIR and Raman spectrum profiles. The FTIR spectra of the prepared glasses consist of BO_3 trigonal and BO_4 tetrahedral units while TeO_2 changes to TeO_3 andTeO_4 structural units. The fraction of N_4 four coordinated boron atoms decreases with increasing BaO as the consequence of BO_4 units turning into asymmetric BO_3 units with increasing (NBOs). The Raman spectra also evident that the replacement of BaO with TeO_2 decreases the concentration of Te–O–Te linkages within the volume of host glass which results in to increase in the concentration of Ba–O–Te linkages along with BO_3 units. Due to this, the overall glass formers connectivity decreases which intern to the creation of NBOs. These glasses, particularly BTBiBV-5 exhibit a unique combination of high refractive index, low phonon energy, and excellent thermal stability. Additionally, the incorporation of vanadium oxides allows for tunable optical properties, making them highly desirable for various technological applications. Various applications like lasers, sensors, medical imaging, nuclear waste storage, batteries, and medical implants.

Acknowledgements The authors express their gratitude to Princess Nourah bint Abdulrahman University Researchers Supporting Project Number (PNURSP2024R26), Princess Nourah bint Abdulrahman University, Riyadh, Saudi Arabia. Dr. B. Srinivas and Dr. Ashok Bhogi would like to thank the Principal and Management of VNR VJIET, Bachupally, Hyderabad for their constant support and encouragement.

Author contributions Writing the first draft of the manuscript and reviewing-editing were performed by B. Srinivas, Khadijah Mohammedsaleh Katubi, Ashok Bhogi, Sheik Ahammed, T.V. Surendra, Abdul Hameed, Md. Shareefuddin, M. S. Al-Buriahi. All authors reviewed the manuscript.

Funding Open access funding provided by the Scientific and Technological Research Council of Türkiye (TÜBİTAK). Princess Nourah bint Abdulrahman University Researchers Supporting Project Number (PNURSP2024R26), Princess Nourah bint Abdulrahman University, Riyadh, Saudi Arabia.

Data availability The data that support the findings of this study are available from the corresponding author upon reasonable request.

Code availability Not applicable.

Declarations

Conflict of interest The authors declare no competing interests.

Ethical approval Not applicable.

Consent to participate Not applicable.

Consent for publication Not applicable.

References

Abdelghany, A.M.: The elusory role of low level doping transition metals in lead silicate glasses. SILICON **2**, 179–184 (2010)

Abdelghany, A.M.: Novel method for early investigation of bioactivity in different borate bio-glasses. Spectrochim. Acta Part A Mol. Biomol. Spectrosc. **100**, 120–126 (2013)

Abdelghany, A.M., ElBatal, H.A.: Optical and μ-FTIR mapping: a new approach for structural evaluation of V_2O_5-lithium fluoroborate glasses. Mater. Des. **89**, 568–572 (2016)

Abdelghany, A.M., Hammad, A.H.: Impact of vanadium ions in barium borate glass. Spectrochim. Acta Part A Mol. Biomol. Spectrosc. **137**, 39–44 (2015). https://doi.org/10.1016/j.saa.2014.08.012

Ahamad, M.N., Varma, K.B.R.: Structural and optical properties of (100–x) $Li_2B_4O_7$·× ($Ba_5Li_2Ti_2Nb_8O_{30}$) glasses and glass nanocrystal composites. Dalton Trans. **39**(19), 4624–4630 (2010)

Ahammed, S., Srinivas, B., Shareefuddin, M., et al.: A comparative study on the physical and spectral (optical, EPR and FTIR) properties of NaF–CdO–B_2O_3 and KF–CdO–B_2O_3 glass systems doped with manganese ions. J. Non Cryst. Solids. **594**, 121789 (2022)

Al-Harbi, F.F., Prabhu, N.S., Sayyed, M.I., Almuqrin, A.H., Kumar, A., Kamath, S.D.: Evaluation of structural and gamma ray shielding competence of Li_2O-K_2O-B_2O_3-HMO (HMO = SrO/TeO_2/PbO/Bi_2O_3) glass system. Optik (2021). https://doi.org/10.1016/j.ijleo.2021.168074

Altowyan, A.S., Abouhaswa, A.S., Sayyed, M.I., Mahmoud, K.A., Al-Hadeethi, Y.: Fabrication, structure, physical and optical features of the 50B_2O_3 + 25Bi_2O_3 + (25–x) Li_2O + xSrO_2 glasses. Optik (2021). https://doi.org/10.1016/j.ijleo.2021.167485

Bhogi, A., Kistaiah, P.: Structural and optical properties of CuO doped lithium borate glasses. Phys. Chem. Glas J. Glas Sci. Technol. Part B **56**(5), 197–202 (2015)

Bhogi, A., Srinivas, B., Papolu, P., Shareefuddin, M., Kistaiah, P.: Effect of Mn^{2+} ions on spectroscopic and electrical properties of lithium strontium borate glasses. Mater. Chem. Phys. **291**, 126698 (2022a)

Bhogi, A., Srinivas, B., Padmavathi, P., et al.: Absorption spectrum fitting method (ASF), DASF method and structural studies of Li_2O–SrO–B_2O_3–MnO quaternary glass system. Opt. Mater. **133**, 112911 (2022b)

Culea, E., Pop, L., Bosca, M., Dan, V., Pascuta, P., Rada, S.: Structural and physical characteristics of xGd_2O_3 (100–x)[Bi_2O_3 B_2O_3] glasses. J. Phys. Conf. Ser. **182**, 12062 (2009)

Davis, E.A., Mott, N.: Conduction in non-crystalline systems V. Conductivity, optical absorption and photoconductivity in amorphous semiconductors. Philos. Mag. **22**(179), 903–922 (1970)

Dimitrov, V., Komatsu, T.: Classification of simple oxides: a polarizability approach. J. Solid State Chem. **163**(1), 100–112 (2002)

Elbatal, H.A., Abdelghany, A.M., Ghoneim, N.A., Elbatal, F.H.: Effect of 3d-transition metal doping on the shielding behavior of barium borate glasses: a spectroscopic study. Spectrochim. Acta Part A Mol. Biomol. Spectrosc. **133**, 534–541 (2014). https://doi.org/10.1016/j.saa.2014.06.044

Fernández Navarro, J.M., Toudert, J., Rodríguez-Lazcano, Y., Maté, B., De Castro, M.J.: Formation of subsurface silver nanoparticles in silver-doped sodium-lead-germanate glass. Appl. Phys. B Lasers Opt. **113**(2), 205–213 (2013). https://doi.org/10.1007/s00340-013-5458-6

Gautam, C., Yadav, A.K., Singh, A.K.: A review on infrared spectroscopy of borate glasses with effects of different additives. ISRN Ceram. **2012**, 1–17 (2012)

Ghoneim, N.A., ElBatal, H.A., Abdelghany, A.M., Ali, I.S.: Shielding behavior of V_2O_5 doped lead borate glasses towards gamma irradiation. J. Alloys Compd. **509**(24), 6913–6919 (2011)

Hall, D.W., Newhouse, M.A., Borrelli, N.F., Dumbaugh, W.H., Weidman, D.L.: Nonlinear optical susceptibilities of high-index glasses. Appl. Phys. Lett. **54**(14), 1293–1295 (1989)

Hameed, A., Srinivas, B., Edukondalu, A., Shareefuddin, M., Chary, M.N.: EPR studies of strontium alkali borate glasses doped with vanadium. Phys. Chem. Glas Eur. J. Glass Sci. Technol. Part B **56**(6), 263–266 (2015). https://doi.org/10.13036/17533562.56.5.263

Hameed, A., Balakrishna, A., Srinivas, B., Chandrasekhar, M., Shareefuddin, M., Chary, M.N.: Influence of manganese ions on physical and spectroscopic properties of mixed alkali-alkaline earth oxide borate glasses. Optik **246**, 167810 (2021)

Herzfeld, K.F.: On atomic properties which make an element a metal. Phys. Rev. **29**(5), 701 (1927)

Jambhale, V.N., Chanshetti, U.B.: Synthesis and characterization of boro-aluminotellurite glass system. J. Chem. Chem. Sci. **8**, 199–203 (2018)

Kashif, I., Soliman, A.A., Farouk, H., El-Shorpagy, M., Sanad, A.M.: Effect of copper addition on density and magnetic susceptibility of lithium borate glasses. Phys B Condens Matter. **403**(21–22), 3903–3906 (2008)

Krishnan, M.L., Neethish, M.M., Kumar, V.V.R.K.: Structural and optical studies of rare earth-free bismuth silicate glasses for white light generation. J. Lumin. **201**, 442–450 (2018)

Kundu, R.S., Dult, M., Punia, R., Parmar, R., Kishore, N.: Titanium induced structural modifications in bismuth silicate glasses. J. Mol. Struct. **1063**, 77–82 (2014)
Lafi, O.A.: Correlation of some opto-electrical properties of Se–Te–Sn glassy semiconductors with the average single bond energy and the average electronegativity. J. Alloys Compd. **660**, 503–508 (2016)
Lalithaphani, A.V., Srinivas, B., Hameed, A., Chary, M.N., Shareefuddin, M.: Electron paramagnetic resonance spectra of CdO–Al_2O_3–Bi_2O_3–B_2O_3 quaternary glasses containing VO^{2+} ions. In: AIP Conference Proceedings, vol. 1942 (2018)
Laorodphan, N., Pooddee, P., Kidkhunthod, P., Kunthadee, P., Tapala, W., Puntharod, R.: Boron and pentavalent vanadium local environments in binary vanadium borate glasses. J. Non Cryst. Solids **453**, 118–124 (2016)
Maalegoundla, C., Sekhar, K.C., Hameed, A., Srinivas, B., Shareefuddin, M.: Physical and spectroscopic studies of CaF_2–Al_2O_3–Bi_2O_3–B_2O_3–CuO glasses. J. Aust. Ceram. Soc. **58**(4), 1137–1146 (2022)
Majhi, K., Vaish, R., Paramesh, G., Varma, K.B.R.: Electrical transport characteristics of ZnO–Bi_2O_3–B_2O_3 glasses. Ionics **19**, 99–104 (2013)
Marzouk, M.A., ElBatal, H.A., EzzElDin, F.M.: Optical properties and effect of gamma irradiation on bismuth silicate glasses containing SrO, BaO or PbO. Silicon **5**(4), 283–295 (2013). https://doi.org/10.1007/s12633-013-9160-4
Marzouk, M.A., ElBatal, F.H., ElBatal, H.A.: Effect of TiO_2 on the optical, structural and crystallization behavior of barium borate glasses. Opt. Mater. **57**, 14–22 (2016)
Montemore, M.M., van Spronsen, M.A., Madix, R.J., Friend, C.M.: O_2 activation by metal surfaces: implications for bonding and reactivity on heterogeneous catalysts. Chem. Rev. **118**(5), 2816–2862 (2017)
Naresh, P., Srinivas, B., Sreenivasu, D., et al.: Preparation and characterization of melt derived CaO–Sb_2O_3–Li_2O containing borate glass for multiple application. J. Non Cryst. Solids **589**, 121642 (2022)
Pascuta, P., Borodi, G., Culea, E.: Structural investigation of bismuth borate glass ceramics containing gadolinium ions by X-ray diffraction and FTIR spectroscopy. J. Mater. Sci. Mater. Electron. **20**, 360–365 (2009)
Pavani, P.G., Sadhana, K., Mouli, V.C.: Optical, physical and structural studies of boro-zinc tellurite glasses. Phys. B Condens. Matter. **406**(6–7), 1242–1247 (2011)
Richards, B., Jha, A., Tsang, Y., et al.: Tellurite glass lasers operating close to 2 μm. Laser Phys. Lett. **7**(3), 177–193 (2010)
Richards, B.D.O., Jha, A., Jose, G., Teddy-Fernandez, T., Binks, D., Tsang, Y.: Tellurite glass as a solid-state mid-infrared laser host material. In: Mid-Infrared Coherent Sources; MW1C-7 (2013).
Shaaban, E.R., Shapaan, M., Saddeek, Y.B.: Structural and thermal stability criteria of Bi_2O_3–B_2O_3 glasses. J. Phys. Condens. Matter **20**(15), 155108 (2008)
Shamshad, L., Rooh, G., Kirdsiri, K., et al.: Effect of alkaline earth oxides on the physical and spectroscopic properties of Dy^{3+}-doped Li_2O-B_2O_3 glasses for white emitting material application. Opt. Mater. **64**, 268–275 (2017). https://doi.org/10.1016/j.optmat.2016.12.027
Srinivas, B., Hameed, A., Shareefuddin, M., Chary, M.N.: EPR and optical studies of BaO–TeO_2–TiO_2–B_2O_3 glasses containing V^{4+} and Cu^{2+} transitional metal ion. Mater. Today Proc. **2**(4–5), 1915–1922 (2015)
Srinivas, B., Hameed, A., Chary, M.N., Shareefuddin, M.: Physical, optical and FT-IR studies of Bismuth-Boro-tellurite glasses containing BaO as modifier. IOP Conf. Ser. Mater. Sci. Eng. **360**, 012022 (2018a). https://doi.org/10.1088/1757-899X/360/1/012022
Srinivas, B., Hameed, A., Ramadevudu, G., Chary, M.N., Shareefuddin, M., et al.: Experimental and theoretical electron paramagnetic resonance and optical studies of Cu^{2+} spin probe in BaO–TeO_2–Bi_2O_3–B_2O_3 glass system. Optik **156**, 289–296 (2018b)
Srinivas, B., Kumar, R.V., Hameed, A., Sagar, D.K., Chary, M.N., Shareefuddin, M.: Physical and optical studies of BaO–TeO_2–TiO_2–B_2O_3 glasses containing Cu^{2+} transition metal ion. In: AIP Conference Proceedings, vol 1953 (2018c)
Srinivas, B., Hameed, A., Vijaya Kumar, R., Narasimha Chary, M., Shareefuddin, M.: Experimental and theoretical investigations on the EPR parameters and molecular orbital bonding coefficients of VO^{2+} ions in BTTB glasses. Philos. Mag. **98**(17), 1625–1640 (2018d). https://doi.org/10.1080/14786435.2018.1450530
Srinivas, B., Hameed, A., Ramadevudu, G., Chary, M.N., Shareefuddin, M.: Evaluation of EPR parameters for compressed and elongated local structures of VO^{2+} and Cu^{2+} spin probes in BaO–TeO_2–B_2O_3 glasses. J. Phys. Chem. Solids **129**, 22–30 (2019)
Srinivas, B., Srikantha Chary, B., Hameed, A., Narasimha Chary, M., Shareefuddin, M.: Influence of BaO on spectral studies of Cr_2O_3 doped titanium-boro-tellurite glasses. Opt. Mater. **109**(August), 110329 (2020). https://doi.org/10.1016/j.optmat.2020.110329

Srinivas, B., Hameed, A., Srinivas, G., Chary, M.N., Shareefuddin, M.: Influence of V_2O_5 on physical and spectral (optical, EPR & FTIR) studies of SrO–TeO_2–TiO_2–B_2O_3 glasses. Optik **225**, 165815 (2021)

Srinivas, B., Bhogi, A., Naresh, P., Hameed, A., Chary, M.N., Shareefuddin, M.: Effect of SrO and TeO_2 on the physical and spectral properties of strontium tellurite boro-titanate glasses doped with Cu^{2+} ions. J. Non Cryst. Solids **575**, 121218 (2022a). https://doi.org/10.1016/j.jnoncrysol.2021.121218

Srinivas, B., Bhogi, A., Naresh, P., et al.: Fabrication, optical and radiation shielding properties of BaO–TeO_2–B_2O_3–Cr_2O_3 glass system. Optik **258**, 168877 (2022b)

Srinivas, B., Chary, M.N., Shareefuddin, M.: Effect of Alkaline earth oxides on the ionic conductivity of boro-tellurite glasses for solid state ion batteries. Phys. Scr. **97**(10), 105812 (2022c)

Stalin, S., Edukondalu, A., Boukhris, I., et al.: Effects of TeO_2/B_2O_3 substitution on synthesis, physical, optical and radiation shielding properties of ZnO–Li_2O–GeO_2–Bi_2O_3 glasses. Ceram. Int. **47**(21), 30137–30146 (2021). https://doi.org/10.1016/j.ceramint.2021.07.192

Suresh, S., Pavani, P.G., Mouli, V.C.: ESR, optical absorption, IR and Raman studies of xTeO_2+(70–x) B_2O_3+ 5TiO_2+ 24R_2O: 1CuO (x= 10, 35 and 60 mol%; R= Li, Na and K) quaternary glass system. Mater. Res. Bull. **47**(3), 724–731 (2012)

Tauc, J.: Amorphous and Liquid Semiconductors. Springer, New York (2012)

Urbach, F.: The long-wavelength edge of photographic sensitivity and of the electronic absorption of solids. Phys. Rev. **92**(5), 1324 (1953)

Vedeanu, N., Stanescu, R., Filip, S., Ardelean, I., Cozar, O.: IR and ESR investigations on V_2O_5–P_2O_5–BaO glass system with opto-electronic potential. J. Non Cryst. Solids **358**(16), 1881–1885 (2012). https://doi.org/10.1016/j.jnoncrysol.2012.05.010

Walia, T., Singh, K.: Mixed alkaline earth modifiers effect on thermal, optical and structural properties of SrO–BaO–SiO_2–B_2O_3–ZrO_2 glass sealants. J. Non Cryst. Solids **564**(March), 120812 (2021). https://doi.org/10.1016/j.jnoncrysol.2021.120812

Yadav, A.K., Singh, P.: A review of the structures of oxide glasses by Raman spectroscopy. RSC Adv. **5**(83), 67583–67609 (2015)

Yadav, A.K., Gautam, C.R., Gautam, A., Mishra, V.K.: Structural and crystallization behavior of (Ba, Sr) TiO_3 borosilicate glasses. Phase Transit. **86**(10), 1000–1016 (2013)